Performance of RC Shallow Beams Externally Bonded with Steel Reinforced Polymer

by Andrea Prota[1], Kah Yong Tan[2], Antonio Nanni[1], Marisa Pecce[3] and Gaetano Manfredi[1]

[1]Dept. of Structural Analysis and Design, University of Naples Federico II, Naples, ITALY
[2]Center for Infrastructure Engineering Studies, University of Missouri-Rolla, Rolla, MO, USA
[3]Dept. of Engineering, University of Sannio, Benevento, ITALY

Abstract

The application of steel reinforced polymer (SRP) in structural strengthening is a new concept based on the use of high-strength steel cord. This paper presents the results of an experimental program on the flexural behavior of reinforced concrete (RC) beams strengthened with SRP, including the performance of epoxy resin versus cementicious grout to impregnate and bond SRP to concrete, as well as the feasibility of nailing the SRP to prevent peeling. The use of cementicious grout is of high relevance as it could allow overcoming the issue of fire resistance and further reduce the cost of the strengthening system. Test results were compared to those from beams strengthened with carbon fiber reinforced polymer (CFRP) under the same experimental program. This preliminary work shows the high potential of SRP strengthening systems and identifies some critical issues that should be investigated next in order to optimize the effectiveness of proposed strengthening solutions.

Keywords: anchorage; cementicious grout; epoxy; fiber reinforced polymer; flexure; reinforced concrete; steel reinforced polymer; strengthening.

Introduction

The steel cord of piano wire used as the reinforcement for radial tires is one of the strongest industrial materials known. It is composed of twisted pearlite steel filaments that have been strengthened by drawing to an ultra fine diameter (0.20~0.35mm) and its strength is higher than alloyed steel containing great amounts of high melting point metal. The use of steel cord to upgrade steel, wood, or concrete members in both new construction and retrofit applications is an emerging new concept in composite reinforcement. The steel cord is varied between the highly twisted cords, for optimum ductility, and slightly twisted cords, which are more open to allow resin penetration, yet maintain cable-like properties. The shape of the steel cord functions the way the threads act on a screw, forming a mechanical interlock to the matrix with short development lengths.

The steel cords are coated with either zinc or brass to enhance corrosion resistance and then aligned and glued on a scrim material to form a very stable and straight steel tape (Hardwire 2002). The steel tape has very high strength and stiffness and is economical to produce. The density of the steel tape ranges from 1.6 to 9 cords per cm (4 to 23 cords per inch) to meet the requirement of reinforcement, viscosity of resin, and cosmetic application. The low-density tape is suitable for light reinforcement, tear resistance and load spreading. It is very permeable and allows for high viscosity resins to be used, including cementicious mixtures and thermoset putties. The high-density tape offers the maximum advantage of the steel fibers and still wets through well with low viscosity resins. No special resin is required for wetting steel cord reinforcement, as it is required for glass and carbon fiber where the fiber sizing plays a critical role. Once the steel tape is impregnated with resin and turns into steel reinforced polymer (SRP), it is well protected and should have satisfactory corrosion resistance (Tashito et al. 1999), however this aspect deserves to be deeply investigated.

Huang et al. (2002) reported on a series of ASTM standard tests of representative SRP specimens. The work included a comparison between theoretical and experimental results. They found that the tensile and compressive moduli in the direction of the steel cord, the in-plane shear modulus, and the tensile axial strength could be accurately predicted by mechanicals of material using micro-mechanical models. The transverse tensile modulus and the Poisson's ratios can also be estimated analytically, though with a smaller accuracy. Unfortunately, the transverse compressive modulus could not be accurately determined from micro-mechanics.

Experimental studies have been carried out on the use of FRP systems for flexural strengthening (Fanning et al. 2001, Brena et al. 2003, Shin and Lee 2003); Alaee and Karihaloo (2003) lately proposed a technique for the repair of flexural members using externally bonded high performance fiber reinforced concrete strips. No systematic test has been conducted yet on concrete elements strengthened using SRP laminates. In order to investigate the flexural behavior of RC beams strengthened with SRP composites, two different types of steel tape with medium and high densities, respectively, were used at University of Naples, Italy, to strengthen seven RC beams using cementicious grout and epoxy resin and tested to failure under static loading system. Arrays of nail anchors were used on two of these beams to fasten the steel tape adhered with cementicious grout in order to prevent peeling. Two additional RC beams strengthened with comparable amount of uni-directional CFRP laminates were tested and compared with those strengthened with SRP composites.

Research Significance

To study the performance and modes of failure of RC beams strengthened with SRP composites using cementicious grout and epoxy resin. The influence of the SRP reinforcement on crack pattern, crack width and spacing are also of interest in this research. The comparison with

results obtained on CFRP strengthened beams allows assessing to which extent SRP could be selected as an alternative solution to FRP; such choice could allow exploiting its advantages related to the use of a cheaper and more ductile reinforcement as well as a traditional and fire resistant matrix. The research demonstrates the feasibility of strengthening RC beams using externally bonded SRP and represents an important step towards the development of a novel strengthening material system for structural upgrade.

Experimental Program

A total of eleven RC shallow beams, 400 x 200 x 3700 mm in size, were cast. The stirrups were ? 8 mm steel bars spaced at 100 mm center-to-center. For all specimens, 2? 8 steel bars were used as compression reinforcement. Five ? 16 were used as tensile reinforcement for the reference beam; for the remaining ten, a loss of steel reinforcement area was simulated by using five ? 10 steel bars as tensile reinforcement. Nine of these beams were strengthened using two different types of steel tape, namely 3X2 cord (i.e., type "A") and 12X cord (i.e., type "B"), and carbon fiber laminates (i.e., type "C"). Figure 1 shows geometric details for the nine strengthened beams. The research program was to test the control beam (i.e., specimen U) and then determine the influence of a reduced steel area equal to 39% (i.e., specimen D) of the control specimen; such loss is rather extreme and it was selected only for setting threshold values. The potential of emerging strengthening techniques to restore the original performance of Beam U was assessed by upgrading the nine remaining beams with reduced internal reinforcement. Depending on type of strengthening material and number of layers different axial stiffness ratios $S= E_{ext}A_{ext}/E_sA_s$ were obtained, where E_{ext} and A_{ext}, and E_s and A_s are the elastic modulus and the total area of externally bonded composites and internal steel bars, respectively. Seven beams were strengthened with steel tapes impregnated with epoxy resin or cementicious grout (i.e., A and B beams); the remaining two

beams (i.e., C-1 and C-2) were strengthened with CFRP laminates impregnated with epoxy resin. Two of the beams strengthened with steel tape using cementicious grout were mechanically anchored with nail anchors (i.e., B-3 and B-4). Table 1 reports the test matrix of the research program, summarizing the area of tensile steel, the type and matrix of the externally bonded reinforcement, and the value of the ratio S. In the last column of the table, the equivalent reinforcement ratio $?_{eq}$ is also reported; it is defined as $?_{eq}=?_s+?_{ext}*E_{ext}/E_s$, where $?_s$ and $?_{ext}$ are the reinforcement ratios of A_s and A_{ext} over the concrete cross sectional area (i.e., width of the cross section times the distance from extreme compression fiber of the centroid of the tensile steel).

Material properties

Concrete cubes were crushed at the time of the beam tests in order to obtain the average cubic strength of each specimen; the average strength of all cubes was very close to 40.1 MPa. Steel bars were also characterized by testing three samples per each diameter. For ? 16 bars average values of 570 MPa, 650 MPa and 12.4% were found for the yield stress, the ultimate stress and the ultimate strain, respectively. For ? 10 bars average values of 500 MPa, 600 MPa and 12% were found for the yield stress, the ultimate stress and the ultimate strain, respectively.

The 3x2 steel cord (Hardwire 2002) is made by twisting 5 individual zinc coated wires together – 3 straight filaments wrapped by 2 filaments at a high twist angle (see Figure 2). The density of the 3X2 tape used in this research program consists of 8.7 cords per cm, which is considered high-density tape. According to the manufacturer it has strength of 13.4 kN/cm.

The 12X steel cord (Hardwire 2002) is made by twisting two different individual brass coated wire diameters together in 12 strands and then over-twisting one wire around the bundle (see Figure 3). The physical ridge provided by the wrap wire works to share load into the matrix and tighten the cord during the tensile loading, further assisting the load transfer to the individual

filaments of the cord. The density of the 12X tape used to strengthen the beams consisted of 6.3 cords per cm, which is considered medium-density tape. According to the manufacturer, it has strength of 7.9 kN/cm and bond-ability to very high viscosity matrix. Table 2 shows the mechanical properties of the steel cords (Hardwire 2002).

The carbon fiber sheet is a unidirectional fiber system with a density of 300 g/m^2. The equivalent fiber thickness is 0.167 mm. According to the manufacturer the ultimate strength and modulus of elasticity related to fiber volume are 4800 MPa and 230 GPa, respectively (Mapei 2000).

A high-performance two-component 100% solid epoxy resin, specially developed for plate bonding applications, was used to bond the steel tape to the concrete substrate (Sika 2000). The technical data of the epoxy resin, supplied by the manufacturer, are shown in Table 3.

The epoxy used to impregnate the dry carbon fiber sheet was also a two-component, medium viscosity, gelatinous solvent-free adhesive (Mapei 2000). Table 3 shows the technical data of the epoxy provided by the manufacturer.

The cementicious grout used to bond the steel tape was a two-component, polymer-modified, pore sealing mortal with the additional benefit of a penetrating corrosion inhibitor (Sika 2000). It has a finishing time of 45 to 60 min. depending on temperature and relative humidity. The technical data of the cementicious grout, supplied by the manufacturer, are shown in Table 4.

The nail anchor was a wide ringed head nylon anchor with zinc plated hammer screw (see Figure 4). The anchor size is 6 mm in diameter and 60 mm long. A 24 mm diameter washer was used to enlarge the ringed head of the anchor in order to obtain a better hold to the steel tape.

Specimen preparation

The bottom face of all beams was sandblasted and cleaned to ensure proper bond before strengthening. No primer was used for bonding SRP tapes with either epoxy or cementicious grout. When a uniform and complete mixing of the epoxy was observed, it was spread to areas where the steel tape had contact. The steel tape was cut into designed length, and pressed into the wet epoxy gel with a hard roller. In the case of two plies of steel tape, an additional layer of epoxy was spread and the previously mentioned steps were repeated. The second ply was started 10 cm from the cut-off point of the first ply.

For beams bonded with cementicious grout the same installation procedure was followed. For beams anchored with nail anchors, a total of 31 holes, 60 mm deep and 6 mm in diameter, were drilled alternatively along two parallel lines, with a center-to-center distance of 200 mm (see Figure 1) prior to strengthening. After bonding the steel tape with cementicious grout, the anchors were hammered into the holes and locked in with 24 mm diameter washers.

The procedure for applying the carbon fiber laminates was as recommended by ACI committee 440 (2002) guideline for externally bonded FRP systems. The surface preparation started with a layer of primer followed by another layer of putty. After the putty had hardened, the carbon fiber sheet was adhered to the surface with the epoxy; then steps similar to those used for the installation of SRP were followed.

Test Setup and Instrumentation

All beams were tested as simply supported members, over a clear span of 340 cm. They were loaded up to failure under a four-point configuration, with a constant moment region of 100 cm across the mid-span (Figure 5). The load was applied through a 500 kN hydraulic actuator and the test was carried out under displacement control.

All beams were instrumented to record global and local parameters. The mid-span deflection was measured by a vertical linear variable displacement transducer (LVDT). Three horizontal LVDTs were placed on one side of the specimen to record displacements over a length of 35 cm across the mid-span. On the opposite side of each beam, crack widths and concrete shortening were measured using demec targets; they were placed 5 cm center to center on a total length of 55 cm at the same depth of the LVDTs on the other side of the beam (Figure 5). Readings were taken at selected load levels as discussed later. A total of 20 strain gages were used during each test to measure strains on the externally bonded reinforcement. Depending on width and number of plies, the strain gage arrangement slightly changed for each beam. In general, some gages were placed within the constant moment region and some at the cut-off points; longitudinal and transverse strain profiles were obtained and will be discussed in following sections.

Test Results

The load-mid-span deflection curves of tested beams are depicted in Figures 6-8, which show the trends of each group of beams strengthened with same material systems compared to the two unstrengthened. Values of loads and mid-span deflections at first cracking (i.e., F_{cr} and $?_{cr}$), yielding of tensile steel bars (i.e., F_y and $?_y$) and ultimate (i.e., F_u and $?_u$) are summarized in Table 5. First cracking of beam U occurred at a load of 13.6 kN; the least amount of tensile reinforcement determined that beam D showed first cracks at a load of about 9.2 kN. After first cracking, a loss of stiffness occurred for both beams; curves highlight a change in slope which is more significant for beam D than for U (Figure 6). The shapes of the load deflection curves indicate another loss of stiffness at loads of 141.4 kN and 43.3 kN for beam U and D, respectively. This is due to yielding of the tensile reinforcement that occurred at mid-span deflections of 35.7 mm and 25.1 mm, respectively. After such thresholds, the behavior of both beams was characterized by large flexural

cracks and then collapse due to concrete crushing in the constant moment region. Failure loads, corresponding to a sudden loss of bearing capacity, were equal to 147.6 kN and 49.3 kN for specimens U and D; their ultimate behavior was characterized by a ductility factor $?_u/?_y$ of 1.6 and 4, respectively.

The installation of the 3x2 steel tape at the bottom of a type D beam was beneficial in terms of first cracking (Figure 6). Regardless of width and number of plies, first cracking of beams A-1, A-2 and A-3 occurred at a load of about 20 kN. A loss of stiffness is then observed; curves show a similar slope for beams A-1 and A-3, which are less stiff than A-2. Then, further loss of stiffness is determined by yielding of the steel bars; A-1 yielded at 60.3 kN, while A-2 and A-3 reached the yielding at loads of 79.7 kN and 76.5 kN, respectively. Plastic branches reflect the different amount of external reinforcement: A-2 and A-3, having the same amount of external steel tape, provide the same slope and are stiffer than A-1. The mode of failure was similar for these three beams; it was concrete cover separation (Figures 9 and 10) which initiated at one of the loading points and caused the separation of the concrete cover up to the depth of the longitudinal steel bars (Teng et al. 2001). The minimum ultimate load within group A beams was provided by A-1 whose failure occurred at about 86.3 kN; the maximum was attained by A-2 which failed at 121.1 kN. The tape layout based on same area as for A-2, but arranged on two plies, limited the ultimate capacity of beam A-3 at 100.4 kN. This specimen exhibited the lower ultimate deflection (i.e., 54.5 mm); despite different ultimate strength, A-1 and A-2 showed similar ultimate deflections of 75.7 mm and 72.4 mm, respectively.

The installation of 12X steel tape did not affect significantly the first cracking of group B beams (Figure 7), whose cracking loads were included in the range 9.2-11.5 kN. However, the corresponding deflections were reduced if compared to that of beam D at same stage (Table 5). The loss of stiffness due to cracking was very similar for beams B-1, B-2 and B-3; such similarity is also

confirmed by very close values of yielding loads ranging between 57.1 and 60.4 kN (Table 5). Beam B-4, having double tape area, was stiffer than the other three and yielded at a load of 75.2 kN. The ultimate behavior highlights that beams B-2 and B-3 failed at loads of 72.7 kN and 71.5 kN, respectively; this points out that the nails were unable to improve the ultimate performance of beam B-3, whose ultimate deflection (i.e., 60.4 mm) was slightly larger than that of B-2 (i.e., 56.8 mm). The epoxy resin allowed beam B-1, whose tape area was the same as for B-2 and B-3, attaining its failure at ultimate load and deflection equal to 88.6 kN and 89.2 mm, respectively. Similar strength performance were attained by beam B-4, whose failure occurred at 86.7 kN. Doubling the tape area enabled B-4 reaching ultimate strength very close to that of an epoxy bonded beam with half tape area (i.e., beam B1), but reduced its ultimate deflection at 46.5 mm. The failure of beams B-1 and B-2 was due to interfacial debonding which initiated at one of the loading points (Teng et al. 2001). The epoxy allowed beam B1 a better engagement of the concrete substrate than that provided by the cementicious grout on beam B2; this can be observed by comparing Figures 11 and 12. The failure of beams B-3 and B-4 was also due to interfacial debonding after nail bearing (Figure 13).

CFRP laminates increased cracking loads of beams C-1 and C-2 (i.e., 13.8 kN and 15.6 kN, respectively) if compared to the unstrengthened beam D (Figure 8). The loss of stiffness due to cracking was more significant for beam C-1 than that of C-2, having double external tape area. This determined also that its yielding load (i.e., 108.6 kN) was higher than that of C-1 (i.e., 75.7 kN). After the yielding point, curves of both specimens show further loss of stiffness that is again more significant for beam C-1 than that of C-2. Both collapsed due to tape debonding initiated at one of the loading points and were characterized by separation of the concrete cover more pronounced for C-2 than for C-1. Even though beam C-2 failed at a load about 40% higher than C-1, their ultimate deflection was almost identical (i.e., 55.8 mm vs. 55.7 mm).

Comparative Discussion of Test Results

The analysis of test results is conducted first with respect to beams strengthened with same external reinforcement (i.e., 3X2 tape, 12X tape and CFRP laminate); then, beams characterized by similar $?_{eq}$ achieved with different externally bonded material are compared. Remarks on the influence of different materials and reinforcement layout on crack widths are also outlined.

For each group of beams strengthened with the same externally bonded material system, the following can be highlighted:

1) up to the yielding of the internal steel rebars, the slopes of the load-deflection curve of beam A-3 are very similar to that of A-1, whose external tape area was half. A-2, equivalent to A-3 in terms of external tape area, exhibited a stiffer behavior prior to steel yielding. This is also evidenced by load-average crack width curves (i.e., average within the constant moment region) depicted in Figure 14. Readings of crack widths were taken manually and only at prefixed stages; that is why values of crack widths were not recorded up to ultimate loads. Curves of Figure 14 confirm that the average crack width was almost identical for beams A-1 and A-3 and it was less than that exhibited by beam A-2. Considering that crack spacing was similar for all tested beams and equal to about the stirrups spacing (i.e., 100 mm), outcomes provided by group A beams suggest that the capability of the externally bonded system to reduce crack width and then stiffen the member in the pre-yielding field is strongly dependent on the width rather than on the sectional area of the bonded steel tape;
2) by doubling the width of the 3X2 steel tape the ultimate strength increased by about 40% (i.e., A-2 vs. A-1), while the ultimate deflection was quite similar. When the same area increase was achieved by doubling the number of plies rather than width (beam A-3) the strength increased only by about 16% if compared to beam A-1 due to a high concentration of interfacial stresses; the ultimate deflection was about 40% larger due to a lower stiffening effect already observed in

the pre-yielding field. Overall, if compared to beam D the 3X2 steel tape provided increases of the ultimate strength ranging between 75% (i.e., A-1) and 145% (i.e., A-2), even though the ultimate deflection had reductions ranging between 25% (i.e., A-1) and 46% (i.e., A-3);

3) no significant stiffening was provided by the 12X steel tape installed on beams B-1, B-2 and B-3 with epoxy and cementicious grout in the pre-yielding field; the load-deflection behavior of beam B-4 appeared slightly stiffer than beam D after a load of about 25 kN. Such result suggest that the structure of the 12X tape makes it less stiff than 3X2 and its capability to reduce crack width (Figure 14) and stiffen the flexural element is negligible;

4) The epoxy resin made beam B-1 able to withstand ultimate load and deflection about 23% and 53% larger than those provided by equivalent beams B-2 and B-3 bonded with cementicious grout, respectively. In order to attain with cementicious grout the strength provided by epoxy resin it was necessary to double the area of 12X tape (i.e., beam B-1 vs. B-4); however, the ultimate deflection of beam B-4 was 48% smaller than that of B-1. The use of nail anchors to improve the bond of the 12X tape was not effective in terms of strength, even though the ultimate deflection of beam B-3 was about 6.5% larger than that of B-2. If compared to beam D schemes based on 12X tape determined strength increase ranging between 46% (i.e., B-3) and 79% (i.e., B-1), with reductions of ultimate deflection ranging between 13% (i.e., B-1) and 55% (i.e., B-4).

5) the installation of CFRP affected the stiffness of strengthened beams and this is confirmed also by crack width trends (Figure 14). By doubling the area of CFRP, the ultimate strength of beam C-2 was about 39% higher than that of C-1; the ultimate deflections were almost identical. If compared to beam D the CFRP reinforcement allowed boosting the strength by percentages ranging between 95% and 173%; a loss of ultimate deflections of 45% was measured for both C-1 and C-2.

The effectiveness of different strengthening solutions can be assessed by comparing flexural members with similar $?_{eq}$ and considering that:

1) slopes of load-deflection curves of beams A-1, B-1, B-2, B-3 and C-1, characterized by $?_{eq}$ ranging between 0.65 and 0.69, are very similar up to yielding of tensile bars. Tape 3X2 impregnated with epoxy (i.e., A-1) was more effective in delaying the first cracking if compared to the CFRP laminate (i.e., C-1). Tape 12X impregnated with epoxy (i.e., beam B-1) or with cementicious (i.e., B-2 and B-3) did not increase the cracking load of the unstrengthened beam D. Branches between first cracking and steel yielding of beams A-1 and C-1 are almost identical; a comparison highlight that both were stiffer than B-1, B-2 and B-3. This can be also observed in terms of load-crack width curves that point out how beams A-1 and C-1 provided almost equal average crack widths and were more capable to reduce crack widths than the other three equivalent beams. (Figure 14). The yielding of steel bars for beams A-1, B-1, B-2 and B-3 occurred at similar loads and deflections (Table 5). The yielding load of beam C-1 was higher by about 29% and corresponded to a similar deflection. Branches of load-deflection curves after steel yielding are about parallel, except for beam C-1 that was stiffer. If impregnated with epoxy, the 12X tape allowed beam B-1 to attain a ultimate deflection about 18% larger that A-1 even though both provided same strength; when it was impregnated with cementicious (i.e. beam B-2) and eventually nailed (i.e., beam B-3) such tape provided ultimate strength and deflection about 16% and 23% smaller than those attained by beam A-1. The use of epoxy to bond the CFRP laminates allowed beam C-1 attaining a ultimate strength about 12% larger than A-1, even though its ultimate deflection was 26% smaller;
2) slopes of load-deflection curves of beams A-2, A-3, B-4 and C-2, characterized by $?_{eq}$ ranging between 0.72 and 0.79, show similar trends up to yielding of internal steel. Tape 3X2

impregnated with epoxy (i.e., A-2 and A-3) was very effective in delaying the first cracking; the CFRP reinforcement had some influence on cracking initiation (i.e., C-2), which was not affected by the installation of tape 12X impregnated with cementicious and anchored with nails (i.e., B-4) (Table 5). Slopes of branches between first cracking and steel yielding highlight a stiffening effect which was maximum for beams A-2 and C-2, decreased for beam A-3 and was not observed in the case of beam B-4. Such trend is confirmed also by a comparison in terms of capacity of the externally bonded system to reduce crack widths (Figure 14). Yielding of steel bars for beams A-2, A-3 and B-4 occurred at similar loads and deflections (Table 5). The yielding of beam C-2 occurred at load and deflection about 41% and 15% higher, respectively. Branches of load-deflection curves after steel yielding are about parallel for beams A-2, A-3 and B-4; beam C-2 provides a stiffer trend that could be partially due to the slight difference of $?_{eq}$ with others (Table 1). The lower bond performance of the cementicious grout affected the strength of beam B-4 which was 71% and 86% that of beams A-2 and A-3 bonded with epoxy resin, respectively. Its ultimate deflection was 65% and 85% that of A-2 and A-3, respectively. The influence of stress concentration that limited the ultimate performance of A-3 (i.e., two plies) if compared to A-2 (i.e., one ply) was already discussed. Beam C-2 provided a strength 11% higher than A-2 with a ultimate deflection 23% smaller. Beams A-2 and C-2 exhibited ultimate strength in the order of 82% and 91% that of beam U, whose $?_{equ}$ was about equal to 2 and 1.9, respectively. This data has particular relevance if one consider that for both A-2 and C-2 the full capacity of the cross-section was not exploited due to debonding of the externally bonded reinforcement. In terms of ultimate deflections, beams A-2 and C-2 attained values equal to 1.26 and 0.98 of that provided by beam D (Table 5).

Conclusions

The paper presents an experimental study aimed at assessing the potential of SRP to provide a strengthening system alternative to traditional techniques and to FRP laminates. SRP-based solutions could utilize improved traditional materials (i.e., steel and cementicious grout). This could be advantageous over FRP and overcome FRP problem areas such as high cost of constituents (fibers and epoxy matrix), fire resistance, low confidence and experience with non-traditional materials, absence of ductility due to fiber linear-elastic behavior, incompatibility with mechanical anchorages due to stress concentration.

Experimental tests were conducted in order to assess the structural effectiveness of SRP and evaluate the influence of epoxy versus cementicious matrix; the possibility of using nail anchors to improve the bond of steel tapes impregnated with cementicious grout was also verified. The performance of seven SRP reinforced beams were compared to that of unstrengthened and FRP reinforced beams. This preliminary analysis of test results underlined that:

1) strength increases provided by SRP bonded with cementicious grout were smaller than those obtained using epoxy. CFRP was more effective than epoxy bonded SRP in terms of strength; the trend was inverted in terms of ultimate deflections. Compared to the unstrengthened beam, SRP allowed attaining strength increases ranging between 46% and 145%, while reductions of ultimate deflections ranged between 13% and 55%. A comparison between beams with equivalent reinforcement ratio highlights that epoxy bonded SRP tapes provided ultimate strength about 10% smaller than CFRP with deflections about 24% larger;
2) the epoxy resin was more effective than cementicious grout in engaging the concrete substrate; regardless of the type of matrix (epoxy or cementicious) the behavior of equivalent (same area of external reinforcement) SRP strengthened beams was similar up to yielding of the internal steel. At ultimate, the epoxy bonded SRP tape determined ultimate strength and mid-span deflection

about 23% and 53% larger than those corresponding to the SRP tape impregnated with cementicious grout;

3) the nail anchors did not affect the performance of the SRP tape impregnated with cementicious grout. The lack of transverse link in the steel tape did not allow distributing the local stress concentration at anchor location; this determined local bearing failure of nails that were unable to improve the bond and delay tape debonding;
4) the 3X2 tape affected the global stiffness of strengthened beams and such effect was dependent on the width rather than on the sectional area of the bonded tape. The different macrostructure made the 12X tape unable to provide any stiffening effect. Such trends were confirmed by recorded widths of cracks, whose spacing was very similar for all tested beams.

Laboratory outcomes confirmed the effectiveness of SRP for the flexural strengthening of RC members. Even though smaller than CFRP, strength increases provided by SRP were significant if compared to upper limits that the strengthening design needs to respect in compliance with ACI 440 (2002) guidelines. Epoxy bonded SRP performed better than FRP in terms of ultimate deflection; this could be very important especially for structures that require an high displacement capacity. Overall, SRP strengthening systems appeared to be a promising technique that could be alternative to FRP when durability is not a critical requirement, even though more research is needed on this aspect. The system could be further optimized by improving the bond of the cementicious grout and by developing effective mechanical anchorages able to prevent or delay delamination. The experimental results presented in the paper could represent a first basis for the development of code recommendations for the design of flexural strengthening of RC structures using SRP.

Acknowledgments

The authors would like to thank Hardwire LLC, Pocomoke City, MD, Mapei Spa, Milan, Italy, and Sika Italia, Milan, Italy, for donating the steel tapes, the FRP system, and the epoxy resin/cementiciuous grout used to bond SRP, respectively.

References

ACI Committee 440, 2002, *Guide for the Design and Construction of Externally Bonded FRP Systems for Strengthening Concrete Structures*, ACI 440-2R.02, American Concrete Institute, Farmington Hills, MI, USA, pp.103.

Alaee, F. J., and Karihaloo, B.L., 2003, "Retrofitting of Reinforced Concrete Beams with CARDIFRC," *ASCE Journal of Composites for Construction*, V. 7, No. 3, pp. 174-186.

Brena, S. F., Bramblett, R. M., Wood, S. L., and Kreger, M. E., 2003, "Increasing Flexural Capacity of Reinforced Concrete Beams using Carbon Fiber-Reinforced Polymer Composites," *ACI Structural Journal*, V.100, No.1,pp. 36-46.

Fanning, P.J. and Kelly, O., 2001, "Ultimate Response of RC Beams Strengthened with CFRP Plates," *ASCE Journal of Composites for Construction*, V.5, No.2, pp. 122-127.

Hardwire LLC, 2002, "What is Hardwire," *www.hardwirellc.com*, Pocomoke City, Maryland.

Huang, X., Birman, V., Nanni, A., and Tunis, 2003, G., "Properties and Potential for Application of Steel Reinforced Polymer (SRP) and Steel Reinforced Grout (SRG) Composites," *Composites, Part B* (accepted for publication).

Mapei, 2000, “World-wide Leader in Products for the Building Indutry”, http://www.mapei.it, Milan, Italy.

Shin, Y., and Lee, C., 2003, “Flexural Behaviour of Reinforced Concrete Beams Strengthened with Carbon Fiber-Reinforced Polymer Laminates at Different Levels of Sustaining Loads,” *ACI Structural Journal*, V.100, No. 2, pp. 231-239.

Sika, 2000, “Sikadur 330, Sika Top 121”, *www.sikausa.com*, Lyndhurst, New Jersey.

Tashito, H., Tarui, T., Sasaki, S., Yoshie, A., Nishida, S., Ohashi, S., Nakamura, K., and Demachi, H., 1999, “Ultra High Tensile Strength Steel Cord,” *Nippon Steel Technical Report No. 80*, Tokyo, Japan, pp. 38-43.

Teng, J.G., Chen, J.F., Smith, S.T., and Lam, L., 2001, *FRP Strengthened RC Structures*, John Wiley & Sons, Ltd, Chichester, England, pp. 245.

List of Tables

List of Figures

Table 1: Test Matrix

Specimen	Tension Steel	External reinforcement	Matrix	Total width (cm)	Plies	S	$?_{eq}$ (%)
U	5? 16	--	---	--	--	--	1.50
D	5? 10	--	---	--	--	--	0.58
A-1	5? 10	Z-3X2	Epoxy	15	1	0.16	0.66
A-2	5? 10	Z-3X2	Epoxy	30	1	0.32	0.74
A-3	5? 10	Z-3X2	Epoxy	30	2	0.32	0.74
B-1	5? 10	B-12X	Epoxy	20	1	0.14	0.65
B-2	5? 10	B-12X	Cement.	20	1	0.14	0.65
B-3 *	5? 10	B-12X	Cement.	20	1	0.14	0.65
B-4 *	5? 10	B-12X	Cement.	40	2	0.28	0.72
C-1	5? 10	Carbon	Epoxy	45	2	0.21	0.69
C-2	5? 10	Carbon	Epoxy	90	3	0.42	0.79

* with nails

Table 2: Material Properties of Steel Cord

Description	Cord Coating	Filament Diameter, mm	Cord Area, mm^2	Cords per cm	Break, N	Elongation, % (Strain to failure)
Z-3X2	Zinc	3 – 0.35, 2 – 0.35	0.48	8.7	1540	2.0
B-12X	Brass	3 - 0.22, 9 - 0.20	0.43	6.3	1250	2.4

Table 3: Mechanical Properties of Epoxy Matrix

Matrix	Tensile Strength, MPa	Elongation, % (Strain at failure)	Flexural Modulus, MPa
SRP-Epoxy	30	1.5	3800
CFRP-Epoxy	30	1.2	3800

Table 4: Mechanical Properties of Cementicious Grout

Matrix	*Flexural Strength, MPa	*Compression Strength, MPa	*Splitting Tensile Strength, MPa	*Bonding Strength, MPa
Cementicious grout	13.8	41.4	5.2	13.8

* Strength at 28^{th} day

Table 5: Summary of Experimental Results

Specimen	F_{cr} (kN)	$?_{cr}$ (mm)	F_y (kN)	$?_y$ (mm)	F_u (kN)	$?_u$ (mm)
U	13.6	1.7	141.4	35.7	147.6	57.1
D	9.2	2.5	43.3	25.1	49.3	102.1
A-1	20.7	5.9	60.3	27.1	86.3	75.7
A-2	20.8	4.5	79.7	29.9	121.1	72.4
A-3	20.1	5.87	76.5	31.5	100.4	54.5
B-1	10.1	1.4	60.4	31.2	88.6	89.2
B-2	10.6	1.8	60.0	33.6	72.7	56.8
B-3	11.5	1.8	57.1	29.9	71.5	60.4
B-4	9.2	1.3	75.2	34.2	86.7	46.5
C-1	13.8	1.9	75.7	31.4	96.5	55.7
C-2	15.6	2.4	108.6	37.0	134.8	55.8

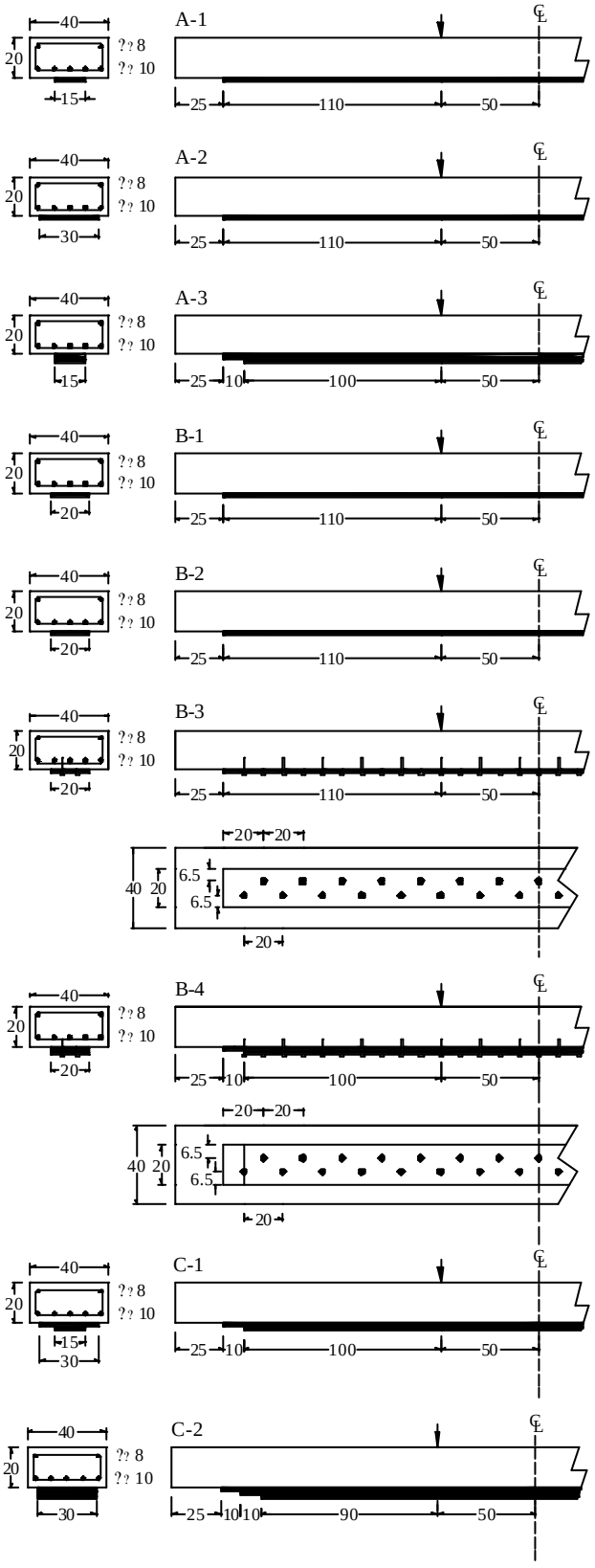

Figure 1: Geometry and Reinforcement of Strengthened Beams (dimension in cm)

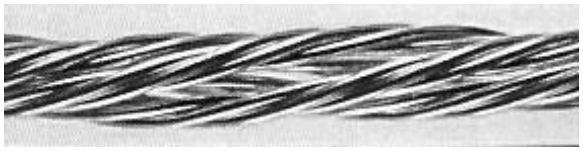

Figure 2: 3x2 cord

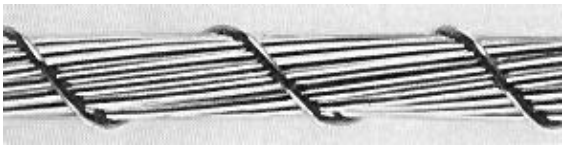

Figure 3: 12x cord

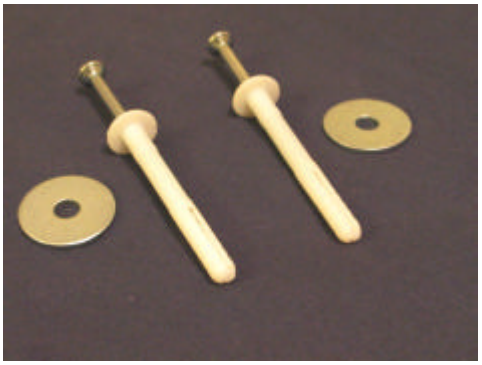

Figure 4: Nail Anchors

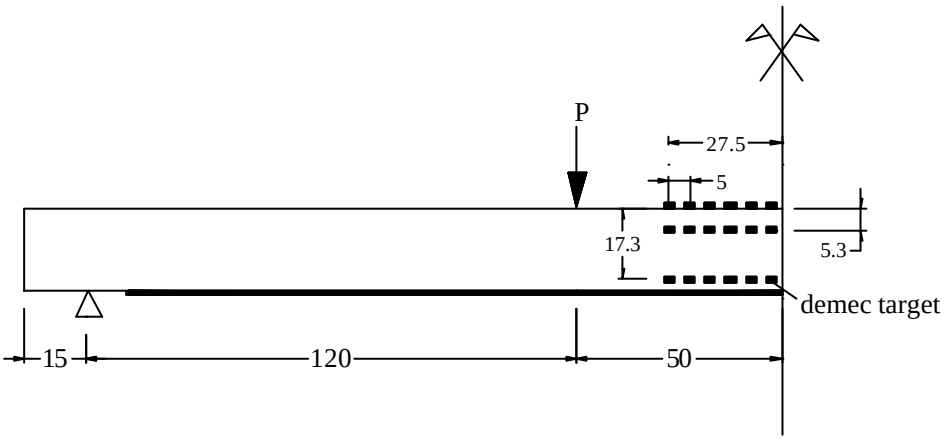

Figure 5: Test Setup (dimensions in cm)

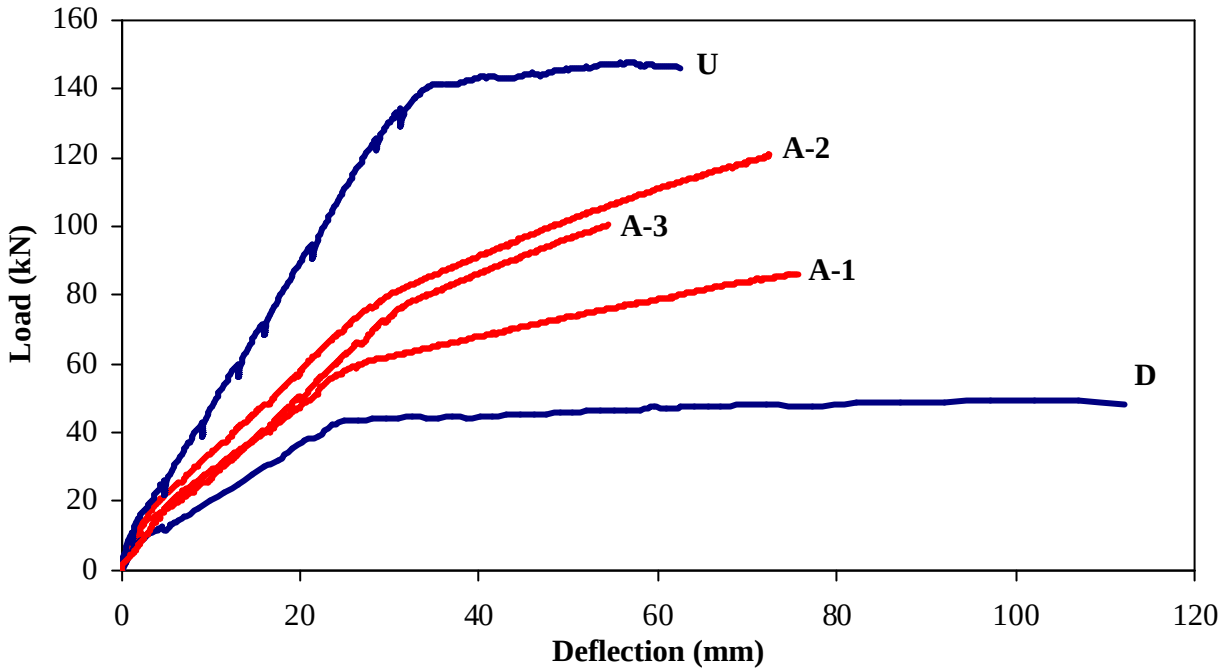

Figure 6: Load-deflection Curves: Control vs. 3X2 Bonded Beams

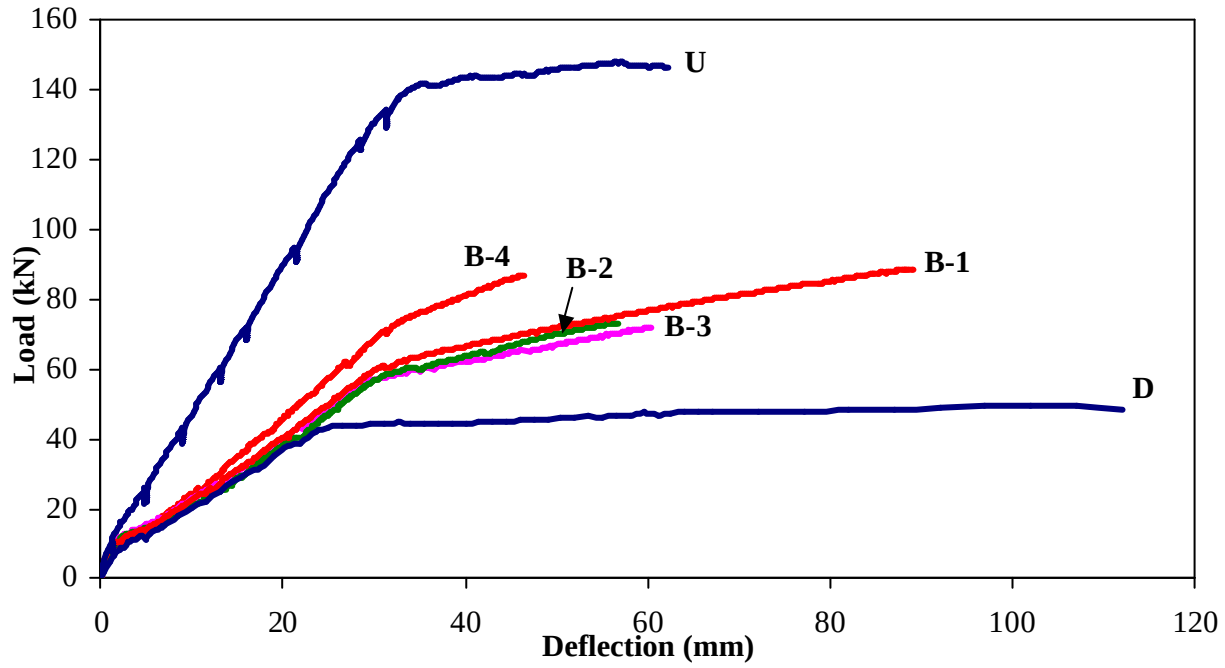

Figure 7: Load-deflection Curves: Control vs. 12X Bonded Beams

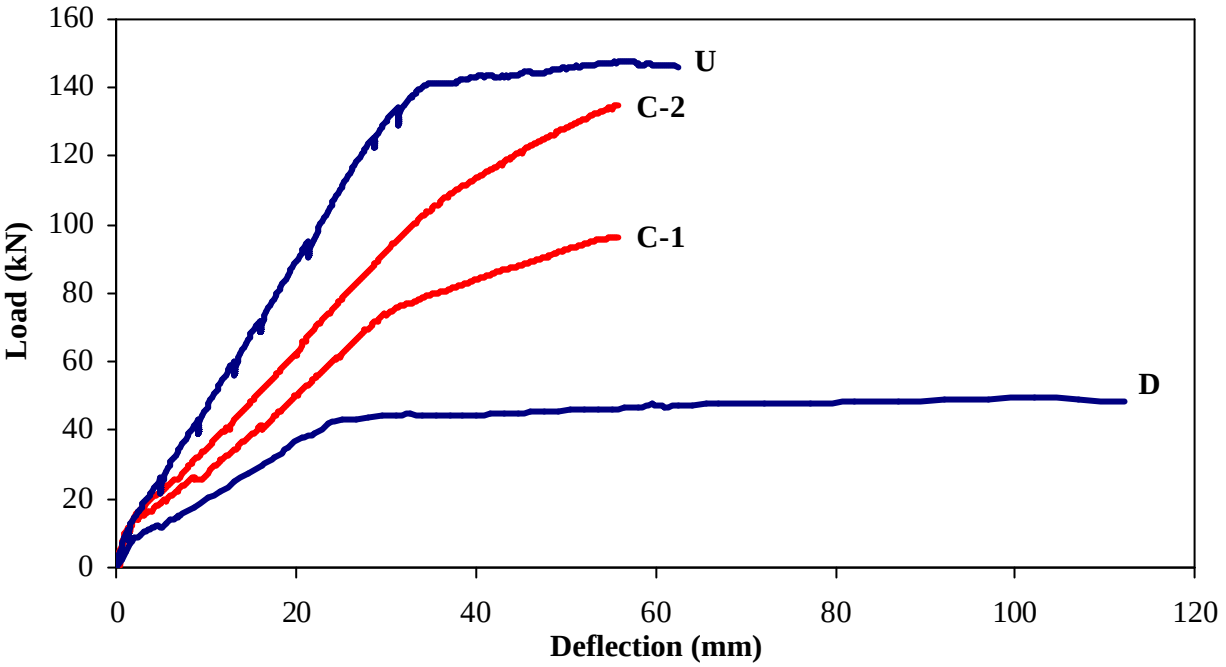

Figure 8: Load-deflection Curves: Control vs. FRP Bonded Beams

Figure 9: Lateral View of Failure of A-2 Beam

Figure 10: Bottom View of Failure of A-2 Beam

Figure 11: Bottom View of Failure of B-1 Beam

Figure 12: Bottom View of Failure of B-2 Beam

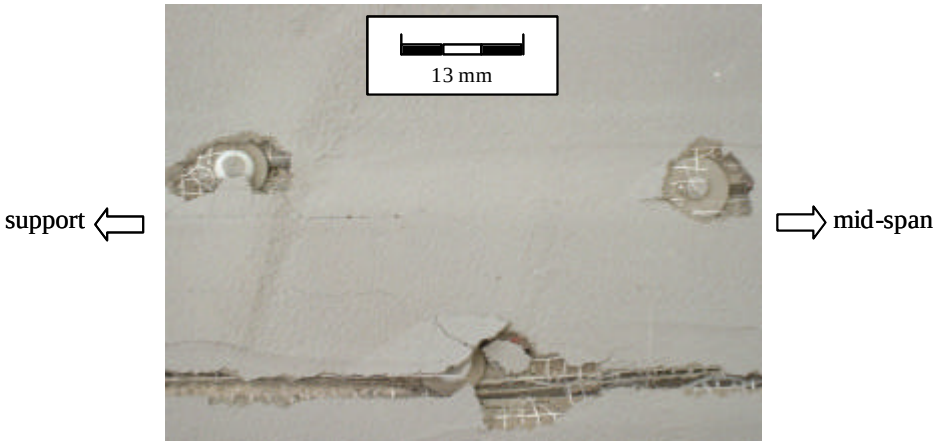

Figure 13: Nail Bearing in Beam B-3

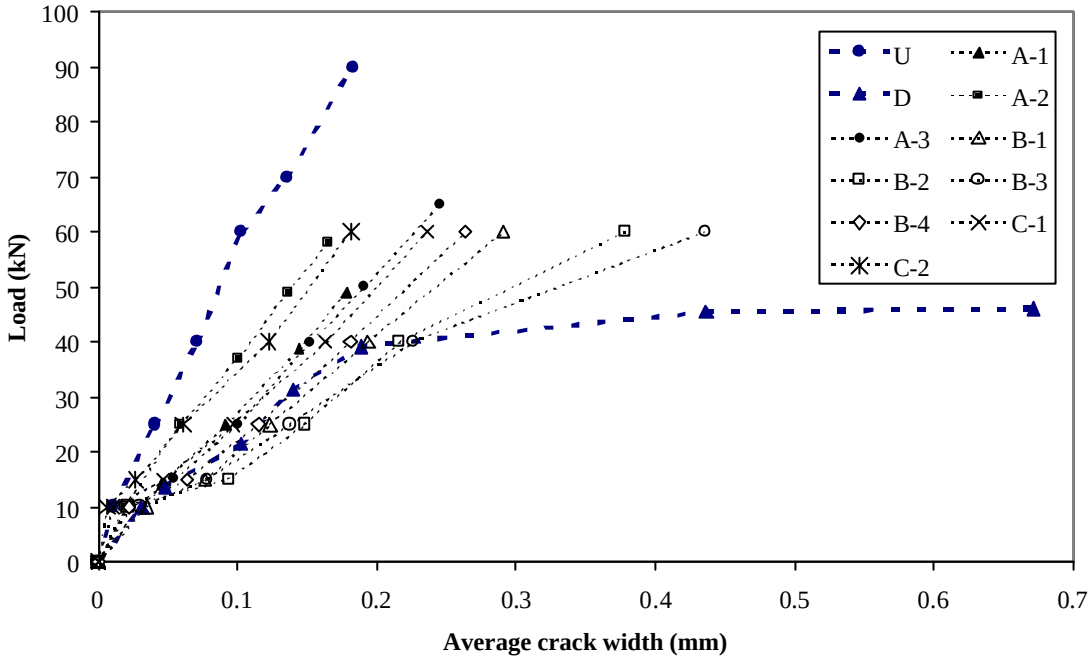

Figure 14: Load vs. average crack width for tested beams